IEEE Access
Multidisciplinary ⋮ Rapid Review ⋮ Open Access Journal

Received October 21, 2020, accepted October 31, 2020, date of publication November 9, 2020, date of current version November 23, 2020.

Digital Object Identifier 10.1109/ACCESS.2020.3036640

Optimal Design and Operation of Regional Multi-Energy Systems With High Renewable Penetration Considering Reliability Constraints

MINGLI ZHANG[1], NA ZHANG[1], DUOJIAO GUAN[2], PENG YE[2], KUN SONG[1], XIAO PAN[1], HUAN WANG[2], AND MENGZENG CHENG[1]

[1]State Grid Liaoning Electric Power Company Ltd., Economic Research Institute, Shenyang 110006, China
[2]Shenyang Institute of Engineering, Shenyang 110136, China

Corresponding author: Duojiao Guan (1586215718@qq.com)

ABSTRACT The regional multi-energy system (RMES) can realize the coupling and complementation of different energy sectors, including electricity, heat, and gas, with the advantage of energy cascade utilization. With the development of hydrogen fuel cell vehicle (FCV) technology, hydrogen has great application potential in the transportation sector. The use of surplus electricity to produce hydrogen through water electrolysis technology can increase renewable energy penetration in power systems. This paper proposed an optimal design and operation method of RMES that considers system reliability constraints under different-level renewable energy penetrations. The RMES includes renewable generation devices, conversion devices such as fuel cells and electric boilers, and emerging devices such as electrolysis cells and hydrogen storage tanks. In order to improve the reliability of the planning results, we consider the reliability constraints of crucial devices in the planning model. In addition, we paid attention to the potential of hydrogen storage tanks for inter-seasonal energy complementation. In the solution of the model, the optimization model can be transformed into a mixed-integer linear programming (MILP) problem by linearizing the non-linear constraints, which can be directly solved by CPLEX, showing good performances in practical applications. Finally, case studies are performed to show the superiority of the planning model.

INDEX TERMS Hydrogen energy, regional multi-energy system, reliability, renewable energy.

I. INTRODUCTION

With the depletion of fossil energy consist of coal and oil and the environmental problem caused by them, people are paying more attention to the development and utilization of renewable energy [1], [2]. Due to the intermittent and fluctuating output of renewable energy, renewable curtailment has become a world problem [3]. The multi-energy system can increase the operational flexibility and economy by hybridizing different technologies, showing great potential in energy supply [4], [5].

From another perspective, the development of water electrolysis and fuel cell technologies makes it possible to convert the redundant power into hydrogen for synthetic ammonia, alcohol production, steel making, fuel cell energy supply, etc. [6]. It gets rid of the single storage function of the battery, realizes the bridge between renewable energy and industrial applications, and can further increase the renewable penetrations [7]. However, as an emerging technology, the longevity and utilization hours of the fuel cells and electrolytic cells are still important issues [8]. Therefore, system reliability must be considered in the design and operation of the RMES.

Up till now, there are some works related to the reliability of the multi-energy system. Based on the energy hub model, the authors of [9] proposed a linearized model for optimal design and operation of multi-energy systems (MES) with reliability requirements, which can satisfy different energy demands while respecting reliability constraints. On this basis, literature [10] further studied the EV integration and low-carbon policy on the optimal design and operation of MES with reliability constraints. In the above research, the expected load not supplied (ELNS), expected energy not supplied (EENS), loss of load expectation (LOLE), and loss of load probability (LOLP) are used to assess the system reliability. The authors of [11] proposed a reliability evaluation model for integrated power-gas systems considering critical

The associate editor coordinating the review of this manuscript and approving it for publication was Jin-Liang Wang.

devices of power-to-gas and gas storage, in which a sequential Monte Carlo (SMC) simulation is utilized to evaluate the system reliability. Furthermore, the authors of [12] used a quasi-sequential Monte Carlo approach to assess system reliability.

The above studies have made significant contributions to the reliability of MES. However, none of them consider the role of hydrogen energy. With the development of water electrolysis technologies, the surplus electricity can be converted into hydrogen through the electrolytic cell (EC) for storage. Then, the hydrogen can further transform into electric power through the fuel cell when there is a shortage in the power supply. More productively, with the application of hydrogen in industrial applications such as synthetic ammonia, oil refining, and emerging transportation demand via fuel cell vehicles, the potential of hydrogen as a terminal energy source is huge [13].

In order to promote the renewable energy penetration, literature [14] proposed an investment-operation model of a multi-stakeholder joint venture consisting of a plant side and a distributed generation side to establish a large-scale hydrogen production plant, achieving win-win cooperation. Literature [15] proposed a planning method for the electricity-hydrogen integrated energy system for high renewable energy penetrations and focused on the functional role of hydrogen energy in inter-seasonal storage. Reference [16] developed an optimal dispatch model of hydrogen energy storage that considers the coupling of transportation and power systems, and studies the value of hydrogen in reducing the price of the electricity market and providing demand response to delay grid expansion planning. Reference [17] proposes a collaborative optimization method of power to hydrogen and heat (P2HH), and the waste heat recovery of EC was considered to improve the conversion efficiency of EC. Reference [18] built a planning model for the liquid organic hydrogen system, which considers the transportation system and electric auxiliary services. The authors of [19] proposed a bi-level optimization model to improve the bidding strategy of power to hydrogen and methane in the multi-energy market and establishes a multi-operation mode model of hydrogen storage to realize the decoupling of hydrogen production and methane production.

The above researches fully affirm the value of hydrogen energy but do not consider the impact of emerging technologies on the safe and reliable operation of the system. Therefore, on this basis, we have further studied the regional multi-energy system (RMES) with high renewable energy penetration and hydrogen utilization. The main contributions are as follows:

1) An optimal design and operation method of RMES considering reliability constraints is firstly proposed, which is beneficial to increase the penetration levels of renewable energy with the consideration of hydrogen-related technologies.
2) A cross-season hydrogen storage model is established to achieve inter-seasonal complementary energy, which shows good performances in improving system economics by the comparative analysis of case studies.

II. SYSTEM STRUCTURE

Fig. 1 shows the structure of the RMES that considers multiple energies, such as electricity, heating, gas, and hydrogen. The RMES consists of photovoltaics (PV), fuel cells (FC), electric boilers (EB), electrolysis cells (EC), batteries (BT), and hydrogen storage tanks (HST). The system can also exchange electric power with the upper grid and purchase natural gas from the gas company to meet the demands of electricity, heating, and hydrogen in this region. The detailed models of all devices are given in the following sections, respectively.

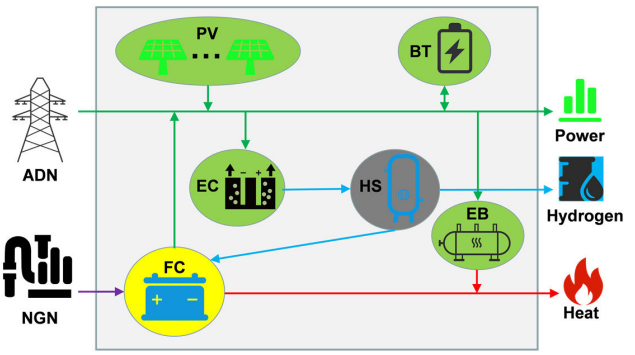

FIGURE 1. Structure of the RMES.

A. ELETROLYZERS

The principle of water electrolysis technology is to use power to drive water into hydrogen and oxygen. Fig. 2 shows the operating mechanisms of electrolysis cells (EC) and fuel cells (FC). At present, alkaline EC, proton exchange membrane (PEM) EC, and solid oxide EC are three main types

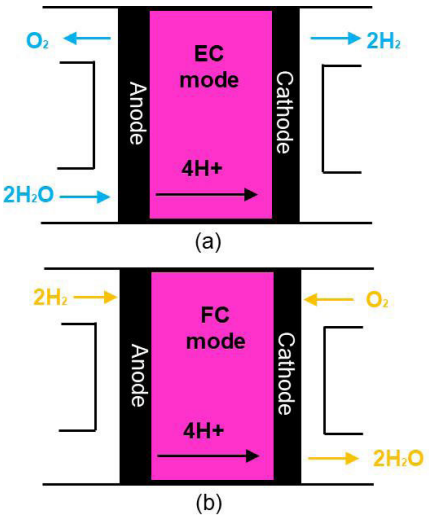

FIGURE 2. Operating mechanisms of EC and FC.

of electrolysis cells, in which the alkaline electrolysis cell is the most mature technology and has reached MW level for industry application, so we use this type of electrolysis cell in this work. The dynamic characteristics of alkaline electrolysis cell are very fast, which can quickly convert excess electricity into hydrogen. Therefore, the alkaline electrolysis cell only needs to meet the following constraints:

$$\xi^{\mathrm{ec}}\varepsilon_{st}^{\mathrm{ec}}\overline{C}^{\mathrm{ec}} \le P_{st}^{\mathrm{ec}} \le \varepsilon_{st}^{\mathrm{ec}}\overline{C}^{\mathrm{ec}} \tag{1}$$

$$H_{st}^{ec} = \eta^{\mathrm{ec}}P_{st}^{\mathrm{ec}} \tag{2}$$

where $\overline{C}^{\mathrm{ec}}$ is the maximum capacity of EC installed in the RMES, $P_{st}^{\mathrm{ec}}$is the input power of EC in scenario s at time t, $H_{st}^{\mathrm{ec}}$is the output hydrogen flow of EC in scenario s at time t, $\varepsilon_{st}^{\mathrm{ec}}$represents the operating states of EC, equaling to 1 if EC works in scenario s at time t, $\eta^{\mathrm{ec}}$is the conversion efficiency of EC, and $\xi^{\mathrm{ec}}$is the minimum load requirement ratio of EC. Constraint (1) represents the maximum and minimum operating constraints of EC, and (2) builds a relationship between input and output of EC.

B. FUEL CELLS

Fuel cells can produce electricity and heat by consuming natural gas or hydrogen. Compared with gas turbines, it has the advantages of fast dynamic response, high electrical efficiency, and low noise emissions [10]. The operating constraints of FC are as follows:

$$\xi^{\mathrm{fc}}\varepsilon_{st}^{\mathrm{fc}}\overline{C}^{\mathrm{fc}} \le P_{st}^{\mathrm{fc,e}} \le \varepsilon_{st}^{\mathrm{fc}}\overline{C}^{\mathrm{fc}} \tag{3}$$

$$-0.5\cdot\overline{C}^{\mathrm{fc}} \le P_{st}^{\mathrm{fc,e}} - P_{s,t-1}^{\mathrm{fc,e}} \le 0.5\cdot\overline{C}^{\mathrm{fc}} \tag{4}$$

$$P_{st}^{\mathrm{fc,h}} = \lambda^{\mathrm{fc}}P_{st}^{\mathrm{fc,e}} \tag{5}$$

$$P_{st}^{\mathrm{fc,e}} = \eta^{\mathrm{fc}}(P_{st}^{gas} + H_{st}^{\mathrm{hcng}}\cdot lhv) \tag{6}$$

$$\begin{cases} 0 \le P_{st}^{\mathrm{hcng}} \le \psi P_{st}^{gas} \\ \psi = \dfrac{11.88\upsilon V}{11.88\upsilon V + 39.05(1-\upsilon)V} \end{cases} \tag{7}$$

where $\overline{C}^{\mathrm{fc}}$ is the maximum capacity of FC installed in the RMES, $P_{st}^{\mathrm{fc,e}}$ and$P_{st}^{\mathrm{fc,h}}$ is the output electric and heating powers of FC in scenario s at time t, andP_{st}^{gas} and H_{st}^{hcng} is the input gas power and hydrogen flow of FC in scenario s at time t, respectively. In addition, η^{fc} is the conversion efficiency, λ^{fc} is the heat-power ratio efficiency, ξ^{fc} is the minimum load requirement ratio, lhv is the lower heat value of hydrogen, ψ and v is the energy ratio and volume ratio of hydrogen enriched compressed natural gas (HCNG), respectively, and V is the volume of the mixture. Constraint (3) represents the maximum and minimum operating constraints of FC, (4) limits the ramping capacity of FC, (5) builds a relationship between the output electric power and heating power, (6) imposes the input and output of FC, and (7) limits the maximum HCNG ratio to ensure the security of FC, and the relationship between ψ and volume ratio v is also given in (7).

C. BATTERIES

Batteries are used to meet the power fluctuation within a day, and its specific constraints are as follows:

$$\begin{cases} 0 \le P_{st}^{bt+} \le \overline{C}_{\mathrm{p}}^{\mathrm{bt}} \\ 0 \le P_{st}^{bt-} \le \overline{C}_{\mathrm{p}}^{\mathrm{bt}} \end{cases} \tag{8}$$

$$0.2\cdot\overline{C}_{\mathrm{e}}^{\mathrm{bt}} \le S_{st}^{bt} \le \overline{C}_{\mathrm{e}}^{\mathrm{bt}} \tag{9}$$

$$S_{st}^{bt} = S_{s,t-1}^{bt} + \left(P_{st}^{bt+}\eta^{bt} - P_{st}^{bt-}/\eta^{bt}\right)\Delta t \tag{10}$$

$$S_{s0}^{bt} = S_{s24}^{bt} \tag{11}$$

where $\overline{C}_{\mathrm{p}}^{\mathrm{bt}}$ and $\overline{C}_{\mathrm{e}}^{\mathrm{bt}}$ are the maximum power-capacity and energy-capacity of BT installed in the RMES, respectively, $P_{st}^{\mathrm{bt+}}$ and $P_{st}^{\mathrm{bt-}}$ are the charging and discharging powers of BT in scenario s at time t, S_{st}^{bt} is the stored electric energy of BT in scenario s at time t, and η^{bt} is the charging/discharging efficiency of BT. Constraint (8) limits the maximum and minimum charging and discharging power of BT, (9) defines the upper and lower stored power of BT, (10) characterizes the dynamical changes of stored electric energy due to the charging and discharging processes, and (11) shows the intraday energy cycles of BT.

D. HYDROGEN STORAGE TANKS

Fig.3 shows the operating mechanism of hydrogen storage tanks (HST). Compared with batteries to meet intra-day power fluctuation, hydrogen storage tanks are mainly used to achieve the energy complementarity between different days or scenarios. From Fig. 3, the stored hydrogen within the HST can be increased if the amount of production is greater than that consumed by FC and FCV in a day or scenario, and vice versa. The operating constraints of HST are listed:

$$S_s^{\mathrm{hst}} = S_{s-1}^{\mathrm{hst}} + \sum_{t\in T}(\eta^{\mathrm{hst}}H_{st}^{\mathrm{ec}} - H_{st}^{\mathrm{hcng}} - H_{st}^{fcv}) \tag{12}$$

$$0 \le S_s^{\mathrm{hst}} \le \overline{C}^{\mathrm{hst}} \tag{13}$$

$$S_0^{\mathrm{hst}} = S_{365}^{\mathrm{hst}} = 0.5\cdot\overline{C}^{\mathrm{hst}} \tag{14}$$

where $\overline{C}^{\mathrm{hst}}$ is the maximum capacity of HST installed in the RMES, S_s^{hst} is the stored hydrogen of HST in scenario s, H_{st}^{fcv} is the hydrogen demand of FCV in scenario s at time t, η^{hst} is the storage efficiency of HST due to the energy consumption

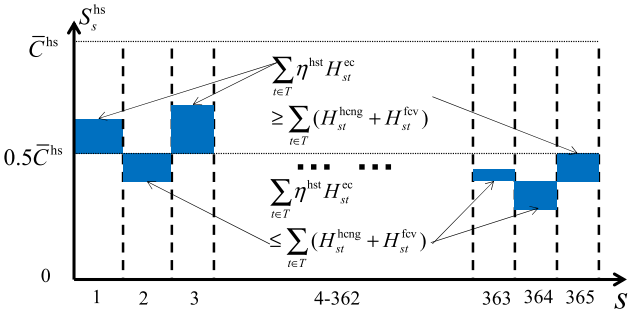

FIGURE 3. Operating mechanism of HST.

for compressing hydrogen, and T is the index for time blocks within a day. Constraint (12) characterizes the dynamical changes of stored hydrogen due to the hydrogen production by EC and hydrogen consumption by FC and FCV. Constraint (13) limits the amount of stored hydrogen in HST, and (14) gives the yearly energy cycle of HST.

E. UPPER GRID AND GAS COMPANY

The interaction with the upper grid and gas company should also be considered as follows:

$$0 \le P_{st}^{grid} \le \overline{P}^{grid} \tag{15}$$
$$0 \le P_{st}^{\text{gas}} \le \overline{P}^{\text{gas}} \tag{16}$$

where $\overline{P}^{\text{grid}}$ and $\overline{P}^{\text{gas}}$ are the maximum interaction power between RMES and upper grid or gas company, P_{st}^{grid} is the purchasing electric power from the upper grid in scenario s at time t, P_{st}^{gas} is the purchasing gas power between RMES and gas company in scenario s at time t.

F. OTHER DEVICES

In addition to the above models, the operating constraints of PV and EB are given in the following:

$$0 \le P_{st}^{\text{pv}} \le p_{st}^{\text{pv}} \overline{C}^{\text{pv}} \tag{17}$$
$$0 \le P_{st}^{\text{eb}} \le \overline{C}^{\text{eb}} \tag{18}$$

where $\overline{C}^{\text{pv}}$ and $\overline{C}^{\text{eb}}$ are the maximum capacity of PV and EB installed in the RMES, p_{st}^{pv} is the unit output power of PV in scenario s at time t, and P_{st}^{pv} and P_{st}^{eb} is the PV output and EB input in scenario s at time t, respectively.

III. OPTIMIZATION MODEL

The optimization model of the RMES that includes objective function, power balances, and reliability constraints is given in this section.

A. OBJECTIVE FUNCTION

The objective function is the total annual cost of the RMES, which consists of the annual investment cost C_{inv} and annual operating cost C_{ope}. The annual investment cost given in (20) includes the annual investment costs of PV, EC, FC, BT, EB, and HS, and the annual operating cost given in (21) includes the annual O&M cost of all components, the annual purchase cost of electricity, and the annual purchase cost of natural gas.

$$\text{Minimize } (C_{inv} + C_{ope}) \tag{19}$$

$$C_{inv} = \frac{r(1+r)^n}{(1+r)^n - 1} \left(\begin{array}{l} c^{\text{pv}}\overline{C}^{\text{pv}} + c^{\text{ec}}\overline{C}^{\text{ec}} + c^{\text{fc}}\overline{C}^{\text{fc}} \\ + c_{\text{p}}^{\text{bt}}\overline{C}_{\text{p}}^{\text{bt}} + c_{\text{e}}^{\text{bt}}\overline{C}_{\text{e}}^{\text{bt}} + c^{\text{eb}}\overline{C}^{\text{eb}} + c^{\text{hs}}\overline{C}^{\text{hs}} \end{array} \right) \tag{20}$$

$$C_{ope} = \sum_{s\in S} \left(\begin{array}{l} \sum_{t\in T} \left(\begin{array}{l} c_m^{\text{pv}} P_{st}^{\text{pv}} + c_m^{\text{ec}} P_{st}^{\text{ec}} + c_m^{fc} P_{st}^{\text{fc}} \\ + c_m^{\text{eb}} P_{st}^{\text{eb}} + c_m^{bt} (P_{st}^{bt+} + P_{st}^{bt-}) \end{array} \right) \\ + \sum_{t\in T} c_{st}^{grid} P_{st}^{grid} + \sum_{t\in T} c^{\text{gas}} P_{st}^{gas} / \eta^{\text{fc}} \end{array} \right) \Delta t \tag{21}$$

where $c^{\text{pv/ec/fc/eb/hs}}$ is the unit investment cost of PV/EC/FC/EB/HS, c_{p}^{bt} and c_{e}^{bt} are the unit investment cost of BT in power and energy capacity, respectively, c pv/ec/fc/eb/bt m is the unit O&M cost of PV/EC/FC/EB/BT, c_{st}^{grid} is the electricity price for purchasing from the upper grid, c^{gas} is the heat price of natural gas. Besides, S is the scenario index.

B. POWER OUTPUTS

Based on the Energy Hub model, the power balances of electricity and heating are given in the following:

$$P_{st}^{grid} + P_{st}^{\text{fc}} + P_{st}^{pv} + P_{st}^{bt-} - P_{st}^{bt+} - P_{st}^{\text{ec}} - P_{st}^{\text{eb}} = P_{st}^{\text{tot},e} \tag{22}$$
$$P_{st}^{\text{fc,h}} + \eta^{\text{eb}} P_{st}^{\text{eb}} = P_{st}^{\text{tot,h}} \tag{23}$$

where $P_{st}^{\text{tot,e}}$ and $P_{st}^{\text{tot,h}}$ are the total output electric and heating powers of RMES in scenario s at time t.

C. RENEWABLE ENERGY PENETRATION

The proportion of renewable energy generation is regarded as an important indicator to measure the advancement of the integrated energy system. Compared with simply using the installed capacity as a percentage of total power generation capacity, the ratio of annual renewable utilization to the total power generation throughout the year can better reflect the actual utilization level of renewable energy generation. To this end, we define the renewable energy penetration ratio as follows:

$$\vartheta = \frac{\sum_{s\in S}\sum_{t\in T} P_{st}^{\text{pv}}}{\sum_{s\in S}\sum_{t\in T} (P_{st}^{\text{pv}} + P_{st}^{\text{grid}} + P_{st}^{\text{fc}})} \tag{24}$$

D. RELIABILITY ASSESSMENT

Four reliability indices are applied in most articles to assess the reliability of the RMES: ELNS, EENS, LOLE, and LOLP. Since the four reliability indices have overlap in characterizing system reliability, we only use ELNS and LOLP in this work. The definition of ELNS and LOLP is as follows:

$$\text{ELNS}^{\vartheta} = \sum_{i\in\Omega}\sum_{s\in S}\sum_{t\in T} \rho_{st}^{i,\vartheta} L_{st}^{i,\vartheta} \tag{25}$$
$$\text{LOLP}^{\vartheta} = \sum_{i\in\Omega}\sum_{s\in S}\sum_{t\in T} \rho_{st}^{i,\vartheta} t_{st}^{i,\vartheta} / 8760 \tag{26}$$

where ϑ means the energy carriers consist of electricity and heating, Ω is the index of all device within the RMES, $\rho_{st}^{i,\vartheta}$ is the probability of failure of device i for producing energy carrier ϑ in scenario s at time t, $L_{st}^{i,\vartheta}$ is the amount of load not supplied due to failure of device i, $t_{st}^{i,\vartheta}$ is the time duration due to failure of device i.

The available reserve of each device i for producing energy carrier $\vartheta$is limited by constraints (27), which imposes the available reserve is non-negative, less than the maximum installed capacity when adding the normal output, and builds a relationship with the total reserve for producing energy

carrier ϑ within RMES.

$$\begin{cases} 0 \le P_{st}^{i,\vartheta} + R_{st}^{i,\vartheta} \le \overline{C}^{i,\vartheta} \\ 0 \le R_{st}^{i,\vartheta} \\ \sum_{i\in\Omega} R_{st}^{i,\vartheta} = R_{st}^{\vartheta-\text{tot}} \end{cases} \tag{27}$$

FOR stands for the equipment forced outage rate, using to statistically calculate the forced unavailability of each device during a long time duration. Actually, the value of FOR is tightly affected by the frequency of use of equipment. Since the longer the equipment is used, the greater the probability of failure, we can suppose that FOR is time-dependent as (28). For instance, Fig. 4 shows the yearly FOR curve of device i, where γ and γ_0 are set to 4 and 15000, respectively [11].

$$\text{FOR}(\gamma) = \frac{1}{1+(\frac{\gamma}{\gamma_0})^{\mu}}, \quad \gamma = 1, 2....8760 \tag{28}$$

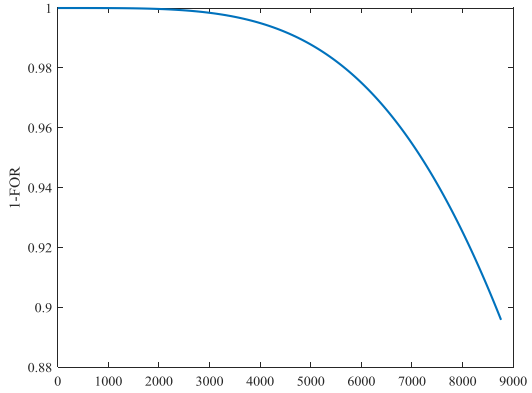

FIGURE 4. Yearly curve of FOR.

The probability of unavailability of each device can be analyzed by its FOR during the planning horizon, given in (29):

$$\rho_{st}^{i,\vartheta} = \text{FOR}^{i,\vartheta} \times \prod_{i\neq i'} (1 - \text{FOR}^{i',\vartheta}) \tag{29}$$

In order to characterize if the unavailability of a device will lead to some loads not supplied, a binary variable $\phi_{st}^{i,\vartheta}$ is defined in (30), equal to 1 if the unavailability of the device i for producing energy carrier ϑ will lead to some loads in scenario s at time t.

$$\frac{L_{tot,t}^{\vartheta} - \sum_{i'\neq i} (P_{st}^{i',\vartheta} + R_{st}^{i',\vartheta})}{\sum_{i\in\Omega} \overline{C}^{i,\vartheta}} \le \phi_{st}^{i,\vartheta} \le 1 + \frac{L_{tot,t}^{\vartheta} - \sum_{i'\neq i} (P_{st}^{i',\vartheta} + R_{st}^{i',\vartheta})}{\sum_{i\in\Omega} \overline{C}^{i,\vartheta}} \tag{30}$$

Then, the ELNS represented in (25) can be re-edited as follows [9]:

$$\text{ELNS}^{\vartheta} = \sum_{i\in\Omega}\sum_{s}\sum_{t} \rho_{st}^{i} \phi_{st}^{i,\vartheta} (P_{st}^{i,\vartheta} + R_{st}^{i,\vartheta} - R_{st}^{\vartheta-\text{tot}}) \tag{31}$$

In the planning model, the calculated ELNS and LOLP should less than the reliability targets.

$$\text{ELNS}^{\vartheta} \le \text{ELNS}^{\vartheta,\text{tar}} = \sum_{i\in\Omega}\sum_{s}\sum_{t} \text{FOR}^{i,\vartheta} \phi_{st}^{i,\vartheta} (P_{st}^{i,\vartheta} + R_{st}^{i,\vartheta} - R_{st}^{\vartheta-\text{tot}}) \tag{32}$$

$$\text{LOLP}^{\vartheta} = \frac{\sum_{i\in\Omega}\sum_{s}\sum_{t} \phi_{st}^{\text{i}} \cdot \text{FOR}^{i,\vartheta}}{8760} \times 100\% \le \text{LOLP}^{\vartheta,\text{tar}} \tag{33}$$

IV. MODEL SOLUTION

A. MODEL LINEARIZATION

There are three types of non-linear terms in the model. The first type is the product-term of binary variable and continuous variable represented by constraints (1) and (3), which can be linearized by the big M method, as follows:

$$\begin{cases} \xi^{\text{ec}} \psi_{st}^{\text{ec}} \le P_{st}^{\text{ec}} \le \psi_{st}^{\text{ec}} \\ -\xi^{\text{ec}} \cdot M \le \psi_{st}^{\text{ec}} \le \xi^{\text{ec}} \cdot M \\ -(1-\xi^{\text{ec}}) \cdot M + \overline{C}^{\text{ec}} \le \psi_{st}^{\text{ec}} \le (1-\xi^{\text{ec}}) \cdot M + \overline{C}^{\text{ec}} \end{cases} \tag{34}$$

$$\begin{cases} \xi^{\text{fc}} \psi_{st}^{\text{fc}} \le P_{st}^{\text{fc}} \le \psi_{st}^{\text{fc}} \\ -\xi^{\text{fc}} \cdot M \le \psi_{st}^{\text{fc}} \le \xi^{\text{fc}} \cdot M \\ -(1-\xi^{\text{fc}}) \cdot M + \overline{C}^{\text{fc}} \le \psi_{st}^{\text{fc}} \le (1-\xi^{\text{fc}}) \cdot M + \overline{C}^{\text{fc}} \end{cases} \tag{35}$$

The second type is the constraint (30) with divisions of optimized variables in upper and lower boundaries. Considering $\phi_{st}^{i,\vartheta}$ is a binary variable, (30) can be changed into (36) by multiply $\sum_{i\in\Omega} \overline{C}^{i,\vartheta}$ in both sides. Then, the non-linear term of $\phi_{st}^{i,\vartheta} \cdot \sum_{i\in\Omega} \overline{C}^{i,\vartheta}$ can be further linearized by the big M method.

$$\begin{aligned} L_{tot,t}^{\vartheta} - \sum_{i'\neq i} (P_{st}^{i',\vartheta} + R_{st}^{i',\vartheta}) &\le \phi_{st}^{i,\vartheta} \cdot \sum_{i\in\Omega} \overline{C}^{i,\vartheta} \\ &\le \sum_{i\in\Omega} \overline{C}^{i,\vartheta} + L_{tot,t}^{\vartheta} - \sum_{i'\neq i} (P_{st}^{i',\vartheta} + R_{st}^{i',\vartheta}) \end{aligned} \tag{36}$$

The last non-linear term is the constraint (32) in characterizing the reliability of RMES, which can further be linearized based on the method proposed in [9], where $\varpi_{st}^{i,\vartheta}$ equals to $\sum_{t} \text{FOR}^{i,\vartheta} \phi_{st}^{i,\vartheta} (P_{st}^{i,\vartheta} + R_{st}^{i,\vartheta} - R_{st}^{\vartheta-\text{tot}})$.

$$\text{ELNS}^{\vartheta} \le ELNS^{\vartheta,\text{tar}} = \sum_{i\in\Omega}\sum_{s}\sum_{t} \varpi_{st}^{i,\vartheta} \tag{37}$$

$$\begin{cases} \mathrm{FOR}^{i,\vartheta}\phi_{st}^{i,\vartheta}(-\sum_{i\in\Omega}\overline{C}^{i,\vartheta}) \\ \le \varpi_{st}^{i,\vartheta} \le \mathrm{FOR}^{i,\vartheta}\phi_{st}^{i,\vartheta}\overline{C}^{i,\vartheta} \\ \varpi_{st}^{i,\vartheta} \le \mathrm{FOR}^{i,\vartheta}(P_{st}^{i,\vartheta}+R_{st}^{i,\vartheta}-R_{st}^{\vartheta-\mathrm{tot}}) \\ \quad +(1-\phi_{st}^{i,\vartheta})\mathrm{FOR}^{i,\vartheta}\phi_{st}^{i,\vartheta}\sum_{i\in\Omega}\overline{C}^{i,\vartheta} \\ \mathrm{FOR}^{i,\vartheta}(P_{st}^{i,\vartheta}+R_{st}^{i,\vartheta}-R_{st}^{\vartheta-\mathrm{tot}})-(1-\phi_{st}^{i,\vartheta}) \\ \mathrm{FOR}^{i,\vartheta}\phi_{st}^{i,\vartheta}\overline{C}^{i,\vartheta} \le \varpi_{st}^{i,\vartheta} \end{cases} \tag{38}$$

B. OVERALL FRAMEWORK

The overall framework of the optimal design and operation model that considers system reliability constraints can be summed up as:

$$\text{Minimize } (C_{inv}+C_{ope}) \quad s.t. \begin{bmatrix} (2),(4)-(18),(20)-(24), \\ (27),(33),(34)-(38) \end{bmatrix} \tag{39}$$

V. CASE STUDIES

A. INITIAL PARAMETERS AND DATA

The RMES shown in Fig. 1 is used to perform the case study. Table 1 shows the efficiency, investment cost, and operation cost of RMES, referenced from [20]–[22]. Fig. 5 shows the annual electric, heating, and hydrogen demands and unit PV outputs. Especially, the annual electric demand comes from actual regional data in northern China, the annual heating demand is simulated by Transient System Simulation Program (TRNSYS) [23], and the unit PV output comes from the National Renewable Energy Laboratory (NREL) [24]. Here, it should be mentioned that we only consider the reliability for supplying heating power (failure of FC and EB), since the RMES can obtain extra electric power when there is a power vacancy due to the unavailability of devices, and the distribution of hydrogen demand within a day is relatively flexible.

TABLE 1. Parameters of RMES.

Equipment	Efficiency	Investment cost	Operating cost
PV	--	8000 ¥/kW	--
EC	0.613	12000 ¥/kW	533.5¥/(kW*year)
HS	0.9	7095 ¥/kg	--
FC	Electricity：0.45 Heat：0.45	10000 ¥/kW	1000¥/(kW*year)
BT	0.95	2265 ¥/kWh 4389¥/kW	70.9¥/(kWh*year) 0.021¥/kW
EB	1	1200 ¥/kW	--

B. ANALYSIS OF DIFFERENT RENEWABLE PENETRATION

Fig. 6 gives the economics of the RMES under different renewable energy penetrations. It can be seen from the figure that as the renewable energy penetration increases, the annual investment cost and annual O&M cost of the system gradually increase, while the annual purchase costs

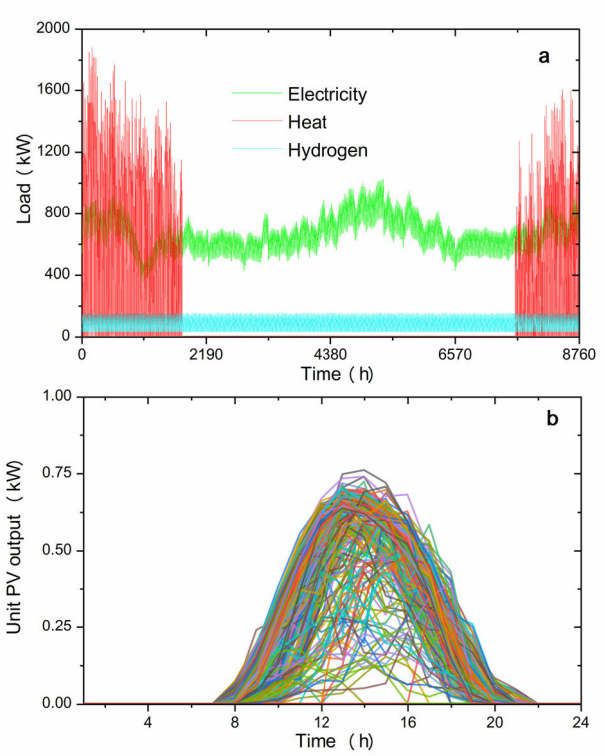

FIGURE 5. Operating mechanism of HS.

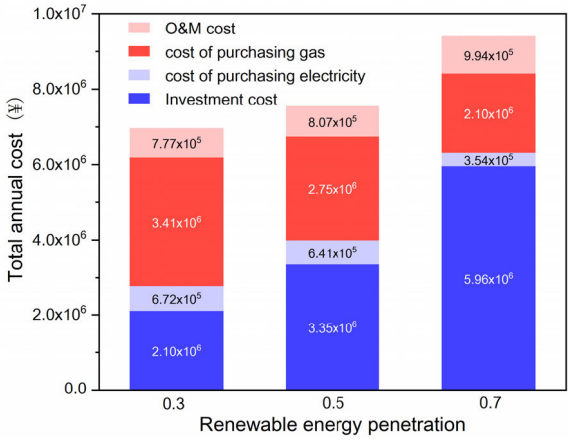

FIGURE 6. Total annual cost under different renewable penetration.

of electricity and natural gas gradually decrease, but the total annual cost of the system clearly increases. Specifically, when the renewable energy penetration is 0.3, the proportion of the annual purchase cost of natural gas is the highest, and when the penetration is 0.7, the annual investment cost of the system is the highest. Fig. 7 shows the equipment configuration results under different renewable energy penetrations. As can be seen from the figure, in order to achieve the renewable proportion requirement, the PV capacity of the system needs to be increased. When the penetration is 0.3, the system will preferentially configure electrolytic cells and

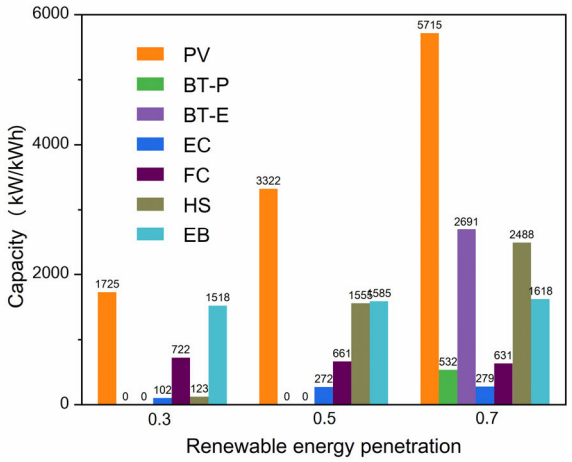

FIGURE 7. Optimal capacity under different renewable penetration.

hydrogen storage tanks instead of BT to achieve photovoltaic consumption. As the penetration increases to 0.7, the system will be equipped with a large number of BT. In addition, as the penetration increases, the installed capacity of FC gradually decreases, while that of EB slightly increases.

C. RELIABILITY ASSESSMENT

Three scenarios are simulated to analyze the reliability effect on the optimal design and operation of RMES. The forced outage rate (FOR) of FC and EB is 0, 2%, and 4% in Scenario 1-3. When the FOR is equal to 0, it means that the unavailability of all devices is not considered. In addition, the reliability targets of $ELNS^{h,tar}$ and $LOLP^{h,tar}$ are set to 1 and 0.1%, respectively, since we consider the reliability for supplying heating power (failure of FC and EB).

Fig. 8 gives the economics of the RMES under different scenarios. It can be seen from the figure that as FOR increases, the total annual cost slightly increases. The reason is as follows. Considering the effect of equipment unavailability, the RMES should install more devices compared with the scenario without reliability constraints. The larger

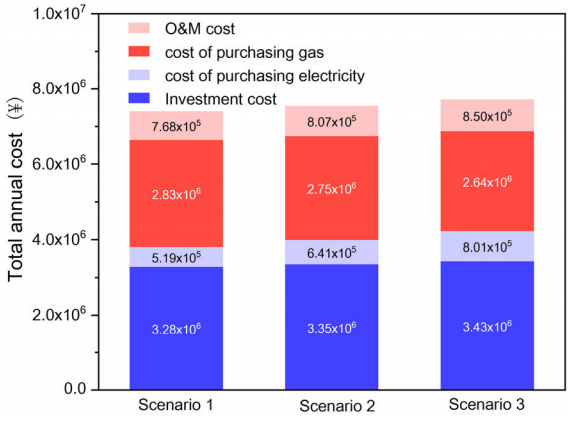

FIGURE 8. Total annual cost under different FORs.

the value of FOR, the higher the probability of equipment failure, so the more equipment capacity the system needs to configure. In addition, the RMES purchases more electricity from the upper grid and less natural gas from the gas company when increasing the value of FOR.

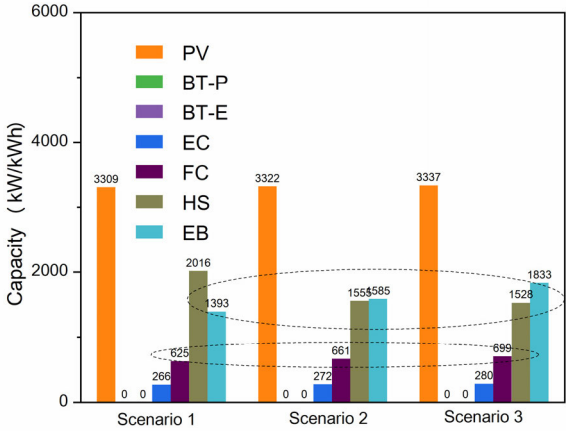

FIGURE 9. Optimal capacity under different FORs.

Fig. 9 shows the device configuration results in three scenarios. From Fig. 9, in addition to the HST, the installed capacity of all devices increase. In particular, due to the failure probability of EB and FC, the capacity of these two devices increase the most, from 625kW and 1393kW in Scenario 1 to 699kW and 1833kW in Scenario 3, respectively. The results show that the introduction of reliability constraints will reduce the economy of the system to a certain extent.

D. OPERATION MECHANISM OF HST

To study the function of HST in the optimal design and operation of RMES, we further compare the total annual cost under scenarios with and without HS, as shown in Fig. 10. As we can see, the total annual cost is higher under the scenario without HS compared with Scenario 2, which highlights the role of HS in improving system economics. Although the investment cost of the RMES under the scenario without HS is relatively low, its annual purchase costs of electricity and natural gas are higher, which leading to an 8% increase in total annual cost compared to Scenario 2. In order to further study the operation mechanism of HST, Fig. 11 gives the daily hydrogen production by EC, HCNG, and hydrogen consumption by FCV within a year. For comparison, the storage state of HST is also plotted in the figure for comparison. It can be seen from the figure that hydrogen production is more volatile than hydrogen consumption. Therefore, HST plays an important role in suppressing the fluctuation of the supply and demand of hydrogen energy. In addition, it can be found from the storage state of HST that HST can realize the cross-day hydrogen energy complementation, and realize a complete round-trip cycle within a time period of tens of days. In addition, the hydrogen flow of HCNG only accounts for a

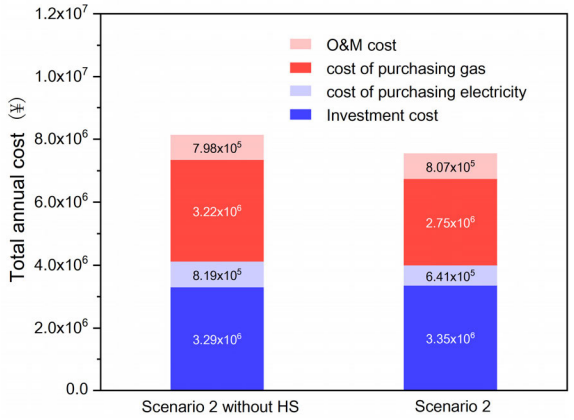

FIGURE 10. Total annual cost under scenarios with and without HS.

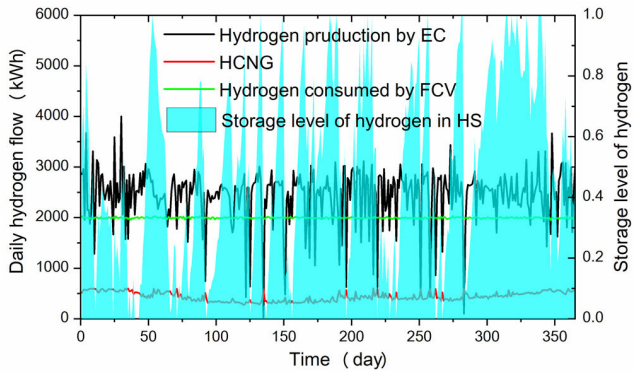

FIGURE 11. Operation results of HST within a year.

small part of the total hydrogen demand due to the limited energy ratio of HCNG. In the future, with technological breakthroughs, a large energy ratio of HCNG or hydrogen fuel cell cogeneration will play an important role in hydrogen applications.

VI. CONCLUSION

In this paper, an optimal design and operation method of regional multi-energy systems that considers system reliability constraints under different-level renewable energy penetrations is proposed. We further established an HST model to achieve the inter-seasonal energy complementation.

The results of the case studies show that the model proposed in this paper is suitable for the planning and design of RMES with different renewable energy penetrations, and the model can satisfy the system reliability requirements. In addition, the system can also consider the integration of emerging technologies, such as HST and HCNG, and FCV.

REFERENCES

[1] E. S. Hanley, J. Deane, and B. Ó. Gallachóir, "The role of hydrogen in low carbon energy futures—A review of existing perspectives," *Renew. Sustain. Energy Rev.*, vol. 82, pp. 3027–3045, Feb. 2018.

[2] J. Yan, S.-K. Chou, U. Desideri, and D.-J. Lee, "Transition of clean energy systems and technologies towards a sustainable future (Part II)," *Appl. Energy*, vol. 162, pp. 1109–1113, Jan. 2016.

[3] B. Yang, X. Cao, Z. Cai, T. Yang, D. Chen, X. Gao, and J. Zhang, "Unit commitment comprehensive optimal model considering the cost of wind power curtailment and deep peak regulation of thermal unit," *IEEE Access*, vol. 8, pp. 71318–71325, 2020.

[4] J. Yu, X. Shen, and H. Sun, "Economic dispatch for regional integrated energy system with district heating network under stochastic demand," *IEEE Access*, vol. 7, pp. 46659–46667, 2019.

[5] G. Pan, W. Gu, Z. Wu, Y. Lu, and S. Lu, "Optimal design and operation of multi-energy system with load aggregator considering nodal energy prices," *Appl. Energy*, vol. 239, pp. 280–295, Apr. 2019.

[6] B. S. Sami, "A survey of hydrogen energy and I-energy applications: Household intelligent electrical power systems," *IEEE Access*, vol. 8, pp. 55181–55203, 2020.

[7] X. Chen, W. Cao, Q. Zhang, S. Hu, and J. Zhang, "Artificial intelligence-aided model predictive control for a grid-tied wind-hydrogen-fuel cell system," *IEEE Access*, vol. 8, pp. 92418–92430, 2020.

[8] U. Javaid, A. Mehmood, A. Arshad, F. Imtiaz, and J. Iqbal, "Operational efficiency improvement of PEM fuel cell—A sliding mode based modern control approach," *IEEE Access*, vol. 8, pp. 95823–95831, 2020, doi: 10.1109/ACCESS.2020.2995895.

[9] A. Shahmohammadi, M. Moradi-Dalvand, H. Ghasemi, and M. S. Ghazizadeh, "Optimal design of multicarrier energy systems considering reliability constraints," *IEEE Trans. Power Del.*, vol. 30, no. 2, pp. 878–886, Apr. 2015.

[10] J. Cao, C. Crozier, M. McCulloch, and Z. Fan, "Optimal design and operation of a low carbon community based multi-energy systems considering EV integration," *IEEE Trans. Sustain. Energy*, vol. 10, no. 3, pp. 1217–1226, Jul. 2019.

[11] Z. Zeng, T. Ding, Y. Xu, Y. Yang, and Z. Dong, "Reliability evaluation for integrated power-gas systems with power-to-gas and gas storages," *IEEE Trans. Power Syst.*, vol. 35, no. 1, pp. 571–583, Jan. 2020.

[12] Z. He, K. Hou, Y. Wang, H. Jia, L. Zhu, Y. Lei, X. Liu, and X. Yu, "Reliability modeling for integrated community energy system considering dynamic process of thermal loads," *IET Energy Syst. Integr.*, vol. 1, no. 3, pp. 173–183, Sep. 2019.

[13] J. Eichman, A. Townsend, and M. Melaina. (Feb. 2016). *Economic Assessment of Hydrogen Technologies Participating in California Electricity Markets*. [Online]. Available: https://www.nrel.gov/docs/fy16osti/65856.pdf

[14] F. Wei *et al.*, "A new equity mode and scheduling strategy of hydrogen production equipment in the multi-subject scene of the grid," *Proc. CSEE*, vol. 38, no. 11, pp. 3214–3225, 2018.

[15] G. Pan, W. Gu, Y. Lu, H. Qiu, S. Lu, and S. Yao, "Optimal planning for electricity-hydrogen integrated energy system considering power to hydrogen and heat and seasonal storage," *IEEE Trans. Sustain. Energy*, vol. 11, no. 4, pp. 2662–2676, Oct. 2020.

[16] N. A. El-Taweel, H. Khani, and H. E. Z. Farag, "Hydrogen storage optimal scheduling for fuel supply and capacity-based demand response program under dynamic hydrogen pricing," *IEEE Trans. Smart Grid*, vol. 10, no. 4, pp. 4531–4542, Jul. 2019.

[17] J. Li, J. Lin, Y. Song, X. Xing, and C. Fu, "Operation optimization of power to hydrogen and heat (P2HH) in ADN coordinated with the district heating network," *IEEE Trans. Sustain. Energy*, vol. 10, no. 4, pp. 1672–1683, Oct. 2019.

[18] N. A. El-Taweel, H. Khani, and H. E. Z. Farag, "Optimal sizing and scheduling of LOHC-based generation and storage plants for concurrent services to transportation sector and ancillary services market," *IEEE Trans. Sustain. Energy*, vol. 11, no. 3, pp. 1381–1393, Jul. 2020, doi: 10.1109/TSTE.2019.2926456.

[19] G. Pan, W. Gu, Y. Lu, H. Qiu, S. Lu, and S. Yao, "Accurate modeling of a profit-driven power to hydrogen and methane plant towards strategic bidding within multi-type markets," *IEEE Trans. Smart Grid*, early access, Aug. 24, 2020, doi: 10.1109/TSG.2020.3019043.

[20] W. Huang, N. Zhang, J. Yang, Y. Wang, and C. Kang, "Optimal configuration planning of multi-energy systems considering distributed renewable energy," *IEEE Trans. Smart Grid*, vol. 10, no. 2, pp. 1452–1464, Mar. 2019.

[21] Committee on Climate Change. (Nov. 2018). *Hydrogen in a Low-Carbon Economy*. [Online]. Available: https://www.theccc.org.uk/publication/hydrogen-in-a-low-carbon-economy

[22] DOE. (Apr. 2019). *Development and Future Prospect of the Hydrogen Fuel Cell Vehicle at Home and Abroad [EB/OL]*. [Online]. Available: https://www.energy.gov/eere/fuelcells/downloads/fuel-cell-technologies-office-multi-year-research-development-and-22.

[23] (Dec. 1983). *Transient System Simulation Program*. [Online]. Available: http://www.transyselectronics.com/
[24] National Renewable Energy Laboratory. (2018). *PVWatts Calculator*. [Online]. Available: http://pvwatts.nrel.gov/pvwatts.php

MINGLI ZHANG received the B.S. degree in electric power system and its automation from Northeast Electric Power University, Jilin, China, in 2005, and the Ph.D. degree from the Shenyang University of Technology, Shenyang, China, in 2013.

He is currently working as a Professor Level Senior Engineer and the Vice-President of Liaoning Electric Power Company Ltd., Economic Research Institute. His research interests include integrated energy system planning, bulk power system planning and operation, and clean energy absorption and application technology.

NA ZHANG received the Ph.D. degree in electric power system and its automation from the Dalian University of Technology, Dalian, China, in 2014. She is currently working as a Senior Engineer and the Vice Director of the Strategic Development Research Center, Liaoning Electric Power Company Ltd., Economic Research Institute. Her research interests include integrated energy system planning, clean energy absorption and application technology, and electric power market.

DUOJIAO GUAN received the master's degree in power engineering from Northeast Electric Power University, in 2003. She currently works as an Associate Professor with the Shenyang Institute of Engineering. Her research interests include plan of integrated energy systems and thermal storage application on power plant.

PENG YE received the Ph.D. degree in electrical engineering from North China Electric Power University, in 2004. He currently works as a Professor with the Shenyang Institute of Engineering. His research interests include integrated energy systems and power system plan and operation.

KUN SONG received the master's degree in power systems and automation from Northeast Electric Power University, in 2007. He was a Senior Engineer, in 2013. His research interests include technology of energy and electricity development and power system planning and design.

XIAO PAN received the Ph.D. degree with the School of Engineering, Warwick University, U.K. He is currently working as a Senior Engineer and the Vice Director of the Strategic Development Research Center, Liaoning Electric Power Supply Company Ltd. His research interests include energy, power strategy planning, clean energy absorption, and application technology.

HUAN WANG received the Ph.D. degree in electrical engineering from the Shenyang University of Technology, Shenyang, China, in 2018. Her research interests include economic optimization of integrated energy systems and planning of power systems.

MENGZENG CHENG received the Ph.D. degree in power systems and its automation from the School of Electronic Information and Electrical Engineering, Shanghai Jiao Tong University, in 2012. He joined State Grid Liaoning Electric Power Company Ltd., Economic Research Institute, in 2012. He directed many technical teams of the Corporation. His research interests include power planning and simulation, integrated energy planning, and company strategic planning.